



Equilibrium, kinetic, and thermodynamic studies on the biosorption of Bordeaux S dye by sericin powder derived from cocoons of the silkworm *Bombyx mori*

Vitor R. Silva^{a,*}, Fabiane Hamerski^a, Thiago A. Weschenfelder^a, Marcelo Ribani^b, Marcelino L. Gimenes^c, Agnes P. Scheer^a

^aChemical Engineering Department, Federal University of Paraná, Francisco H. Santos St., Curitiba, Paraná, Brazil, Tel. +55 41 3361 3584; emails: vrenan@ufpr.br (V.R. Silva), fabianehamerski@gmail.com (F. Hamerski), thiago.weschenfelder@gmail.com (T.A. Weschenfelder), agnesps@gmail.com (A.P. Scheer)

^bTechnology Institute of Paraná, João Américo St., 330 Curitiba, Paraná, Brazil, email: ribani@tecpar.br

^cChemical Engineering Department, State University of Maringá, Colombo Av., 5790 Maringá, Paraná, Brazil, email: marcelino@deq.uem.br

Received 17 July 2014; Accepted 1 December 2014

ABSTRACT

The biosorption of Bordeaux S dye onto sericin powder derived from silkworm cocoons was studied in a batch adsorption system to determine the kinetic mechanism, the equilibrium, and thermodynamic parameters. The Langmuir, Freundlich, and Temkin isotherm models were used for the equilibrium modeling. In order to describe the kinetics, the fits of pseudo-first-order, pseudo-second-order, Weber–Morris, Crank, and external liquid film diffusion models were evaluated. The adsorption occurs favorably at pH below 3.2. The kinetic and equilibrium studies showed fast adsorption and interaction were limited to the monolayer surface, with pseudo-second-order and Langmuir models providing the best fits. Thermodynamic studies indicated that the system is spontaneous and exothermic and that physical interactions govern the adsorption process. The results revealed that sericin powder has the potential to be used as a biosorbent for the treatment of wastewater containing the dye Bordeaux S.

Keywords: Sericin powder; Degumming process; Bordeaux S; Batch adsorption

1. Introduction

The synthetic dye Bordeaux S, commonly referred to as amaranth, is a dye widely used as a coloring agent for textiles, papers, phenol–formaldehyde resins, wood and leathers, and before its legal prohibition to be used as a coloring agent for food and beverages, it was also employed as a food additive in jams, jellies, ketchup, and cake decoration [1,2]. Although its car-

cinogenic nature is still under debate, it has been verified that a high concentration of this dye can adversely affect human/animal health and can cause tumors, and allergic and respiratory problems [2]. Furthermore, the dye content in effluents originating from the food industry, even in low concentrations, may interfere with the passing of light, which, in turn, makes it difficult for the coloring components to be degraded, causing serious adverse effects on the aquatic ecosystems receiving such discharges [3].

*Corresponding author.

The treatment of wastewaters containing dyes involves chemical and physical methods including: coagulation, precipitation, oxidation by ozone, ionizing radiation and membrane filtration, ion-exchange, ozonation, and electrokinetic coagulation. However, these technologies are generally ineffective for color removal, besides being expensive, and they can also result in waste production and present low applicability or adaptability to a wide range of dye containing wastewaters [4,5]. As a viable alternative, biosorption using biomass and biomaterials has received increasing interest owing to its cost-effectiveness, ability to produce less sludge, and environmental friendliness and thus a practical bioprocess for dye-containing wastewater needs to be developed [6,7].

Sericin is a water-soluble globular protein derived from silkworm cocoons. It belongs to a family of proteins with molecular masses in the range of 10–310 kDa and comprises 18 amino acids, most of which have strong polar side groups, such as hydroxyl, carboxyl, and amino groups, being especially rich in aspartic acid and serine, which represent around 19 and 32% of the sericin molar amino acid composition, respectively [8,9]. In general, sericin is discharged in silk-manufacturing wastewater during the silk degumming step where, sericin is removed by partial hydrolysis in the synthetic soap solution (Marseille soap and sodium carbonate, at 95 °C for 1 h) from the silk cocoon, and the natural molecular weight is reduced to 20 kDa [10,11].

However, in recent years, the range of possible applications of sericin that was recovered during the degumming process, along with the natural compound fibroin, has been increasing considerably [12,13]. The recovered sericin, with its natural structure, can be applied in the development of many types of biofilms and structural materials [14,15]. In tissue engineering, sericin with a high molecular weight can be used to induce the oriented crystallization of biomaterials or to improve the biocompatibility of some biomaterials for instance, hydroxyapatite [16,17]. In the development of industrial processes, proteins derived from the silkworm cocoons has been shown to be an interesting natural source material for the development of biofilms applied in membrane processes [18,19] and biosorbents for adsorption processes [20,21].

In this context, we focus on the study of the adsorption of Bordeaux S dye in aqueous solution onto silk sericin powder derived from the degumming of the cocoons of *Bombyx mori* silkworm. To achieve this aim, equilibrium batch experiments were performed and the thermodynamics, equilibrium, and adsorption kinetics were investigated.

2. Materials and methods

2.1. Biosorbent

The biosorbent used in this study was obtained from the process applied for the degumming of silkworm cocoons, according to the methodology described by Silva et al. [22]. The degumming process was conducted by hot water extraction, with cocoons of *Bombyx mori* obtained from the northwest region of Paraná State, Brazil. The cocoons were cut into small pieces to help the extraction and 10 grams of the chopped cocoons were placed in 250 mL of deionized water, in an Erlenmeyer flask, for the degumming process which was carried out in an autoclave (Phoenix, model AV-30, São Paulo, Brazil) at 120 °C for 20 min. Sericin was obtained from the degumming solution by freezing it at –20 °C, followed by lyophilization for 24 h in a compact system (Liotop™, model L101, São Paulo, Brazil). The dried material was ground (Marconi™, model MA630/1, São Paulo, Brazil) for 5 min at 150 rpm to reduce it to a fine powder.

Bordeaux S (trisodium 2-hydroxy-1-(4-sulfonate-1-naphthylazo) naphthalene-3,6-disulfonate, molecular formula $C_{20}H_{11}N_2O_{10}S_3Na_3$), was obtained free of charge from Duas Rodas Company, Brazil. Concentrations of the aqueous dye solution were monitored on a spectrophotometer (FEMTO—model 600 plus) at a wavelength of 520 nm [23]. The pH of the aqueous solution of the dye was adjusted with 0.1 mol L^{-1} HCl or 0.1 mol L^{-1} NaOH, both reagents being of AR grade.

2.2. Biosorbent characterization

The sericin powder obtained from silkworm cocoons of *Bombyx mori* was examined by scanning electron microscopy using a Jeol JSM-6360LV microscope. The surface area was determined by the BET method [24], with nitrogen adsorption/desorption measurements taken at 77.4 K using a Quantachrome™ Autosorb-1 instrument. X-ray diffraction (XRD) data of the sericin powder were collected on a PANalytical X-ray powder diffractometer using Cu K α radiation ($\lambda = 1.5406 \text{ \AA}$, 40 kV and 30 mA), in the 2θ position within the range of 3–70° and with a step size of 0.02. The potential surface charge (Z_p) of sericin at different pH values was determined considering the isoionic point, according to the methodology described by Salis et al. [25].

The silk sericin amino acids and molecular weight profiles were obtained by high performance liquid chromatography (HPLC) and the separation was

carried out on a Merck Hitachi LaChrom system, consisting of an L-7100 quaternary pump, L-7250 programmable auto-sampler, L-7455 diode array detector, and L-7300 column oven. Merck HSM software version 4.1 was used for the data treatment. The amino acids profile was determined using a Waters C-18 column (3.9×150 mm ID, Nova-Pak, end capped, 4 μ m particle size). The mobile phases were water containing acetate buffer at pH 6.4 with acetonitrile:water 94:6 (v/v) (phase A) and acetonitrile:water 60:40 (v/v) (phase B). The sericin molecular weight distribution was measured by size exclusion chromatography on the same HPLC system, with a Waters Ultrahydrogel linear column (300 nm \times 7.8 in), using Pululan polysaccharide as the standard with molecular weights of 20, 50, 100, 200, 400, and 800 kDa.

2.3. Batch adsorption studies

The batch adsorption experiments were carried out in a temperature-controlled orbital shaker (TecnalTM TE-421, Sorocaba, Brazil) at a constant speed (150 rpm) and at three controlled temperatures ($20.0 \pm 0.5^\circ\text{C}$, $30.0 \pm 0.5^\circ\text{C}$, and $40.0 \pm 0.5^\circ\text{C}$). In each test, 30 mL of an aqueous solution of Bordeaux S was placed into a 125 mL conical flask with 0.030 ± 0.005 g of biosorbent, and the flasks were hermetically sealed. The uptake of Bordeaux S dye at time t , q (mg g^{-1}), was obtained through the mass balance, according to the Eq. (1):

$$q = \frac{[C_o - C] \cdot V}{w} \quad (1)$$

where V (mL) is the solution volume, C_o (mg L^{-1}) is the initial concentration of Bordeaux S dye, C (mg L^{-1}) is the liquid-phase concentration of Bordeaux S dye at time t (min), and w (g) is the mass of the biosorbent.

2.4. Adsorption kinetic models

In this study, five kinetic models were used to fit the experimental adsorption kinetics data. They are: the pseudo-first-order, pseudo-second-order, Weber–Morris intraparticle diffusion, Crank, and external liquid film diffusion models.

The pseudo-first-order Eq. (2) and pseudo-second-order Eq. (3) models assume that the adsorption mechanism is similar to the chemical reaction process [26], where $q(t)$ and q_{EQ} are the amount of Bordeaux S adsorbed onto sericin at time (t) and at equilibrium, respectively, and K_1 and K_2 are the kinetic constants

of the pseudo-first-order and pseudo-second-order models, respectively.

$$\frac{dq(t)}{dt} = K_1 \cdot (q_{\text{EQ}} - q(t)) \quad q(0) = 0 \quad (2)$$

$$\frac{dq(t)}{dt} = K_2 \cdot (q_{\text{EQ}} - q(t))^2 \quad q(0) = 0 \quad (3)$$

The diffusion models used in this study were the Weber–Morris intraparticle diffusion Eq. (4) and Crank Eq. (5) models. As reported by Qiu et al. [27], these models consider that the restrictive adsorption mechanism involves the diffusion of the liquid film surrounding the solid surface through the internal pores of the adsorbent.

$$q(t) = K_W \cdot \sqrt{t} \quad (4)$$

$$q(t) = q_{\text{EQ}} \cdot \left\{ 1 - \frac{6}{\pi^2} \cdot \sum_{n=1}^{\infty} \frac{1}{n^2} \cdot \exp(-n^2 \cdot K_D \cdot t) \right\} \quad (5)$$

where K_W and K_D are the diffusion constants of the Weber–Morris and Crank models, respectively.

The external liquid film diffusion model adopted, was described by Puranik et al. [28]. This model is generally used to describe the mass transfer from the bulk of the liquid through the liquid film surrounding the solid surface Eqs. (6) and (7).

$$\frac{dC(t)}{dt} = K_{\text{TM}} \cdot (C(t) - C_1(t)) \quad C(0) = C_o \quad (6)$$

$$\frac{dC_1(t)}{dt} = \frac{V \cdot K_{\text{TM}}}{w \cdot q_M \cdot K_L} \cdot (1 + K_L \cdot C_1(t))^2 \cdot (C(t) - C_1(t)) \quad C_1(0) = 0 \quad (7)$$

where $C(t)$ and $C_1(t)$ are the Bordeaux S concentration in the bulk solution and in the liquid film surrounding the sericin surface, respectively, and K_{TM} is the convective mass transfer coefficient.

2.5. Adsorption equilibrium

The adsorption capacity of an adsorbent can be described by its equilibrium sorption isotherm, which is characterized by certain constants whose values express the surface properties and the affinity of the adsorbent with the solute.

The Langmuir isotherm is a non-linear model which assumes that the monolayer uptake of the solute is on a homogeneous surface, with uniform adsorption energy for all binding sites and with no interaction between the adsorbed molecules [29]. The model is given in the Eq. (8)

$$q_{\text{EQ}} = \frac{q_{\text{M}} \cdot K_{\text{L}} \cdot C_{\text{EQ}}}{1 + K_{\text{L}} \cdot C_{\text{EQ}}} \quad (8)$$

where q_{EQ} (mg g^{-1}) is the amount adsorbed at equilibrium, C_{EQ} is the equilibrium concentration of the Bordeaux S dye (mg L^{-1}), K_{L} is Langmuir equilibrium constant (L mg^{-1}), and q_{M} is the maximum adsorption capacity of the adsorbent (mg g^{-1}).

The empirical Freundlich isotherm [29] is obtained based on the assumption that the sorption takes place on a heterogeneous adsorbent surface, where the sorption energy distribution decreases exponentially. This equation is also applicable to multilayer adsorption and is expressed by the Eq. (9)

$$q_{\text{EQ}} = K_{\text{F}} \cdot C_{\text{EQ}}^{\frac{1}{n}} \quad (9)$$

where K_{F} is the Freundlich constant and n is the heterogeneity factor. The K_{F} value is related to the adsorption capacity and the n^{-1} values indicate the adsorption intensity.

The Temkin isotherm considers the effect of indirect interactions between the adsorbate molecules. This model assumes that adsorption is characterized by a uniform distribution of binding energies, up to a maximum binding energy, and the heat of adsorption of all molecules in the layer decreases linearly with the degree of cover, due to adsorbent–adsorbate interactions. The Temkin isotherm is given by Eq. (10):

$$q_{\text{EQ}} = \frac{R \cdot T}{b} \cdot \ln (K_{\text{T}} \cdot C_{\text{EQ}}) \quad (10)$$

where K_{T} (L g^{-1}) is the Temkin constant, R is the ideal gas constant ($8.314 \text{ J mol}^{-1} \text{ K}^{-1}$), T is the adsorption temperature, and b is related to the heat of adsorption.

2.6. Estimation of thermodynamic parameters

The thermodynamic parameters of the adsorption were determined from equilibrium constants (K_{EQ}), i.e. the constants corresponding to the distribution of the solute between the solid and liquid phases at equilibrium for each temperature. Equilibrium constants, for each temperature, were calculated according to the

method of Khan and Singh [30]. The standard Gibbs free energy (ΔG_{ADS}) of adsorption was calculated according to Eq. (11). The slope and intercept of the Van't Hoff equation, along with the corresponding plots of $\ln (K_{\text{EQ}})$ vs. T^{-1} Eq. (12) were used to determine the enthalpy (ΔH_{ADS}) and entropy (ΔS_{ADS}) of adsorption:

$$\Delta G_{\text{ADS}} = -R \cdot T \cdot \ln K_{\text{EQ}} \quad (11)$$

$$\ln K_{\text{EQ}} = \frac{\Delta S_{\text{ADS}}}{R} - \frac{\Delta H_{\text{ADS}}}{R \cdot T} \quad (12)$$

2.7. Validating the kinetic and isotherm models

The parameters and coefficients of determination (R^2) of the kinetic and isotherm models were obtained by non-linear least squares regression analysis considering a 95% confidence interval. The Levenberg–Marquardt algorithm was employed as the interactive method and the StatSoft™ STATISTICA software (version 7.0) was used for all calculations. The parameters and predicted values for the external liquid film diffusion model were obtained by stochastic optimization of the simulated annealing algorithm [31], in a computer routine run in Fortran Visual Compaq 6.6. The coefficient of determination (R), sum of the squares of residues (SSR), and mean absolute percentage error (ME) were obtained to determine the validity of the models and to reproduce the experimental data.

3. Results and discussion

3.1. Characterization of the biosorbent

The XRD (Fig. 1) results showed a large peak at 19.2° . According to Lee et al. [32], this peak is characteristic of the conversion of the random coil structure into the β -sheet structure due to intermolecular hydrogen bonding between the hydroxyl groups of the amino acids present in sericin, indicating that the sericin powder obtained from the degumming and freeze-drying processes is insoluble in water. The micrograph of sericin (Fig. 2) shows that the lyophilized sericin degummed without chemicals has a sponge-like thin layer structure without pores, as observed by Lee et al. [32].

The BET analysis indicated that the sericin had a surface area of 18.52 m g^{-1} and pore volume of $2.04 \times 10^{-2} \text{ cm g}^{-1}$, indicating a non-porous morphology.

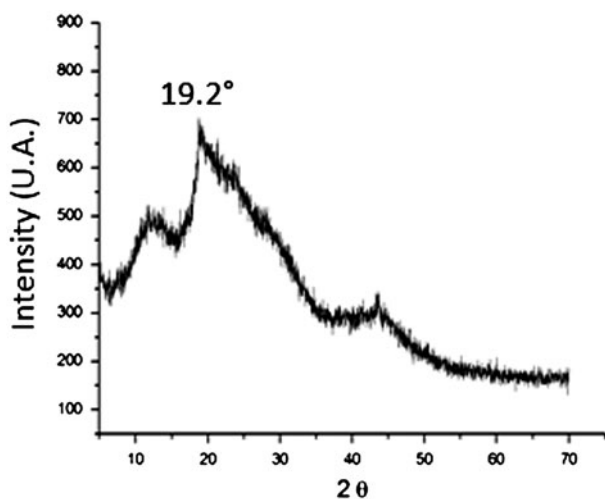


Fig. 1. XRD sericin powder.

Chen et al. [21] used hydrolyzed sericin obtained from a commercial source with a surface area of $1.5 \text{ m}^2 \text{ g}^{-1}$. The sericin powder obtained in this study, applying the hot water process without chemicals, had a higher molecular weight, between 20 and 400 kDa, with a predominant peak at 200 kDa, as shown by the molecular weight profile (Fig. 3), which reveals a larger surface area than the hydrolyzed commercial sericin.

The analysis of the silk sericin to determine the amino acids composition indicated that the major amino acids were glycine (23.20%), serine (21.56%), aspartic acid (14.00%), and arginine (11.95%), respectively. The amount of polar amino acids with hydroxyl groups (serine), acid groups (aspartic acid), and basic groups (arginine) were very high (up to 61.36%) which was similar to the observations of Zhang et al. [8].

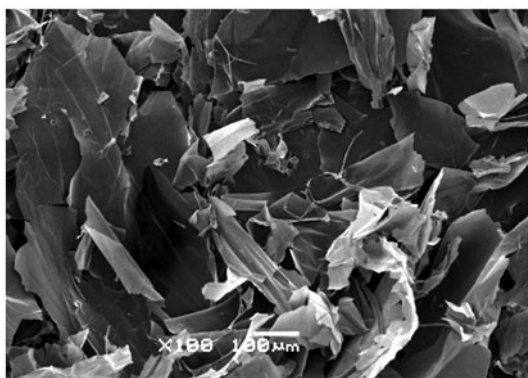


Fig. 2. SEM of silk sericin powder.

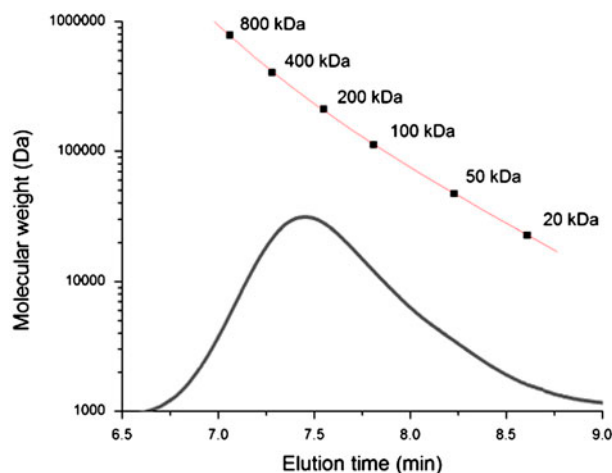


Fig. 3. Molecular weight profile of sericin solution.

3.2. Adsorption studies

The behavior of the Bordeaux S dye adsorption onto silk sericin was studied over a wide range of pH (1.75–8.00) and the findings are shown in Fig. 4. The sericin powder showed biosorption at pH below 3.5, but for pH above 3.5 the adsorption did not occur. A similar result was reported by Mittal et al. [2] who observed that Bordeaux S adsorption onto de-oiled soya and bottom ash occurred only at pH below 3.0

The isoionic point of the sericin indicates neutral charge at pH between 3.20 and 3.35 (Fig. 5) and positive charge at pH lower than 3.20, with the protonation of the amide groups ($-\text{NH}_2$) and some functional groups of the polar amino acids, such as arginine ($=\text{NH}_2^+$). The Bordeaux S adsorption onto sericin powder occurs due to the interaction between the

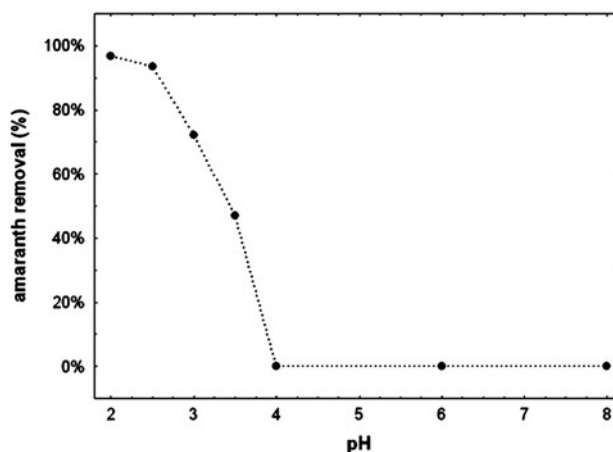


Fig. 4. Effect of pH on Bordeaux S biosorption.

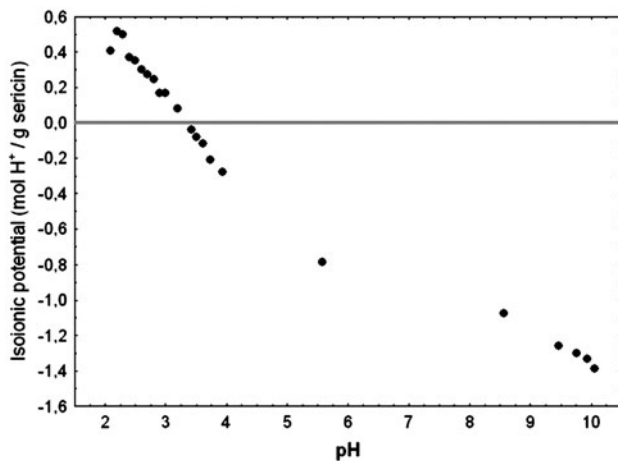


Fig. 5. Isoionic potential of sericin against pH.

positive charges of the surface amino acids, at pH below the isoelectric point, and the negative charge of the sulfonate group of the acid dye ($-\text{SO}_3^-$). Therefore, the kinetics and equilibrium studies were conducted at pH 2.0.

3.3. Adsorption kinetics

The kinetics of the adsorption of Bordeaux S onto sericin was measured through the curves of the adsorption capacity as a function of time at pH 2.0 with a dye concentration of 300 mg L^{-1} and the capacity for biosorption onto sericin was observed at different temperatures. As shown in Fig. 6, independently of the temperature applied, the adsorption of the Bordeaux S dye onto the sericin powder was a fast process, with a high amount of dye adsorbing within the first 10 min of contact. However, after the first 10 min, the adsorption rate decreased over time until saturation of the silk sericin was reached. After 180 min, the percentage removal of Bordeaux S solution was between 65.3 and 72.7%, for an initial Bordeaux S concentration of 300 mg L^{-1} in a batch process with 30 mL of solution and 30 mg of sericin powder.

The adsorption process at 20°C showed the best performance with an average mass of Bordeaux S dye adsorbed of $214.06 \pm 3.06 \text{ mg g}^{-1}$. For 30 and 40°C , the corresponding values were 197.98 ± 2.36 and $192.03 \pm 2.46 \text{ mg g}^{-1}$, equivalent to 7.5 and 10.3% less than the value obtained at 20°C , respectively. This slight reduction in the adsorption performance can be attributed to the destabilizing of the electrostatic interactions between the sericin functional groups and the sulfonate group of the dye as the temperature increased.

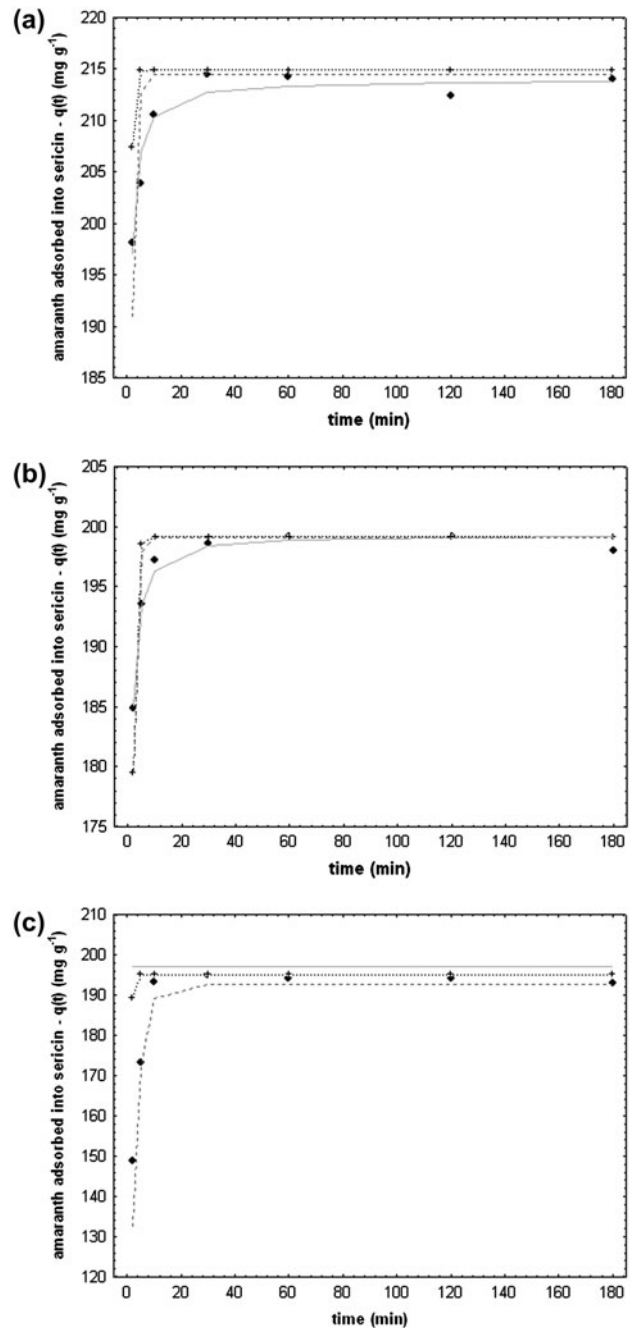


Fig. 6. Kinetics of Bordeaux S adsorption by silk sericin. (a) $T = 20^\circ\text{C}$, (b) $T = 30^\circ\text{C}$, (c) $T = 40^\circ\text{C}$ experimental data (●), pseudo-first-order (···+···), pseudo-second-order (—), and Crank model (---).

Table 1 reports the kinetic parameters of the Bordeaux S adsorption onto the sericin powder. It was observed that the pseudo-second-order model provided a good fit with the experimental data, with R values of 99.72–99.99%, the lowest residual values (SSR) of between 2.44 and 87.35, and mean errors

Table 1
Kinetic parameters of Bordeaux S adsorption onto sericin powder

Kinetic models		20°C	30°C	40°C
Pseudo-first-order model	K_1	1.26 ± 0.13	1.31 ± 0.67	0.67 ± 0.06
	q_{MAX}	214.49 ± 0.87	199.15 ± 7.47	195.10 ± 3.16
	SSR	138.33	34.17	254.09
	R^2	99.78	99.93	99.34
	EM	0.10	0.05	0.15
Pseudo-second-order model	$K_2 \times 10^2$	2.72 ± 0.28	3.25 ± 0.15	0.81 ± 0.01
	q_{MAX}	213.99 ± 0.14	199.37 ± 0.06	197.16 ± 0.13
	SSR	15.54	2.44	87.35
	R^2	99.96	99.99	99.72
	EM	0.04	0.02	0.10
Intraparticle diffusion Weber–Morris model	K_W	23.18 ± 4.94	21.59 ± 4.64	20.87 ± 4.14
	SSR	89,317	78,801	62,829
	R^2	26.66	25.69	34.63
	EM	3.45	3.45	3.40
	Intraparticle diffusion Crank model	K_C	0.86 ± 0.11	0.91 ± 0.07
q_{MAX}		214.95 ± 4.75	199.12 ± 7.47	192.8 ± 3.46
SSR		706.29	533.78	733.78
R^2		98.52	98.76	98.67
EM		0.11	0.07	0.16
External liquid film diffusion model	$K_{TM} \times 10^2$	1.66 ± 0.01	1.65 ± 0.01	1.63 ± 0.01
	SSR	8,129	6,734	3,771
	R^2	96.56	95.82	96.45
	EM	0.66	0.74	0.61

(ME) of 2–10%. The pseudo-second-order model assumes that the adsorption occurs due to the difference between the concentrations at the adsorbate surface and in solution, and mass transfer is limited only by external resistance. Due to the specific morphology (non-porous) and the selective interaction between the protonated functional groups of the sericin and the negatively charged sulfonate groups of the Bordeaux S dye, the interaction is specific and superficial and external mass transfer is predominant. Therefore, the superficial models showed the best fit for the kinetic behavior of Bordeaux S biosorption onto sericin.

The Weber–Morris model provided very low R values, between 25.69 and 34.63% and the highest SSR (62,829–89,317), and EM (3.40–3.45) values. This indicates that internal mass transfer is not a relevant resistance mechanism. The Crank diffusion model approaches the pseudo-first- and pseudo-second-order models, but this model did not describe the initial transient adsorption.

The external liquid diffusion model describes the external mass transfer between the bulk liquid and the liquid film surrounding the solid surface, considering equilibrium at the interface. Fig. 7 shows the kinetics predicted by this model and as with the pseudo-first-order and pseudo-second-order models, the profile indicates a fast adsorption process reaching

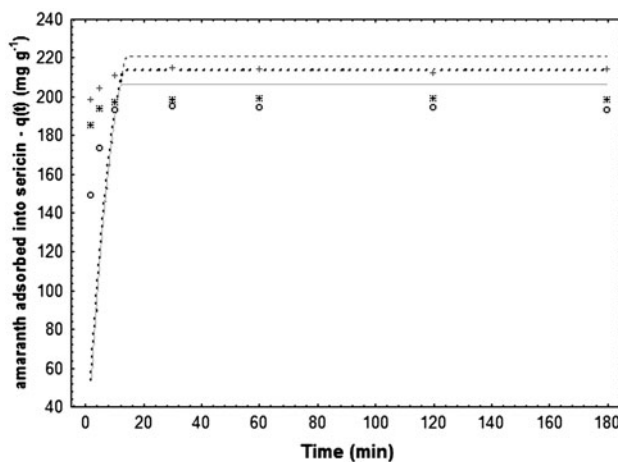


Fig. 7. External mass transfer kinetics: Fit curves at 20°C (···), 30°C (- - -), and 40°C (—), experimental data at 20°C (+), 30°C (*), and 40°C (°).

equilibrium after 10 min. Fig. 8 shows the estimated Bordeaux S dye concentrations in the bulk liquid and in the liquid film surrounding the particle surface for each temperature evaluated and for all temperatures, the Bordeaux S dye concentrations in the bulk liquid and film liquid approach equilibrium after 10 min, when the kinetics model reaches the equilibrium.

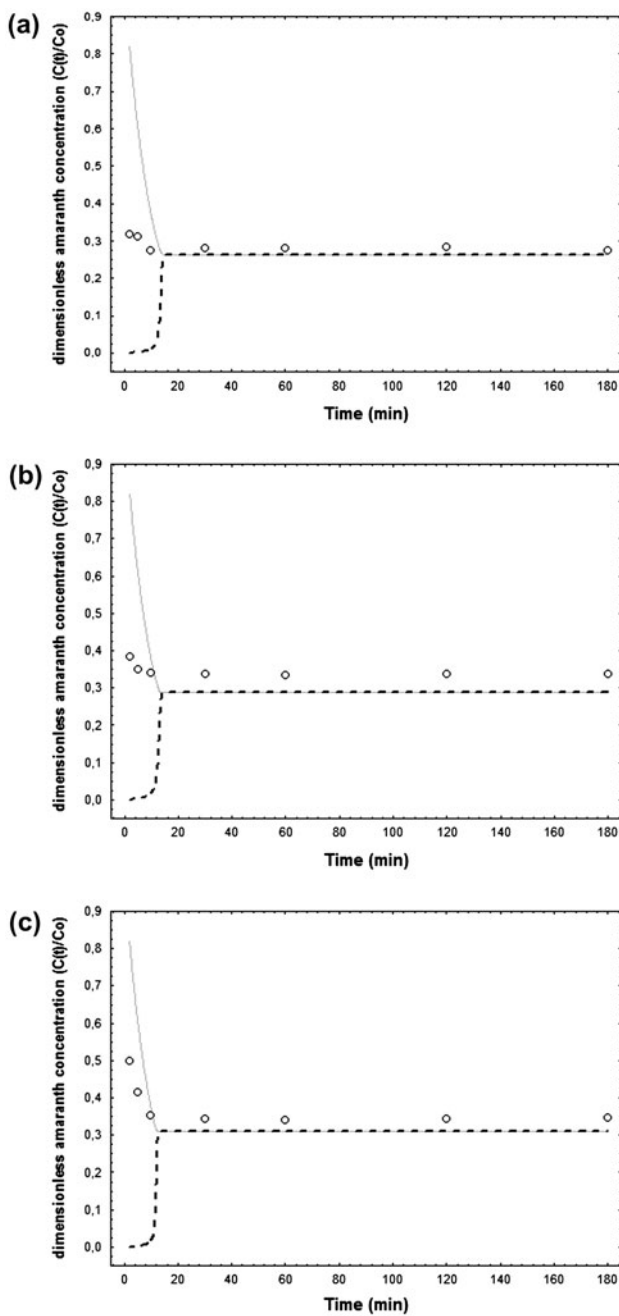


Fig. 8. Dye concentration at film surrounding the particle (---) and bulk liquid (—) for 20°C (a), 30°C (b), and 40°C (c) and experimental values of dye concentration at bulk liquid (○).

3.4. Adsorption equilibrium and thermodynamic parameters

Equilibrium adsorption isotherms provide very important information for the design and implementation of adsorption processes. Thus, to better understand the adsorption process, the Langmuir, Freundlich, and Temkin isotherms were applied in

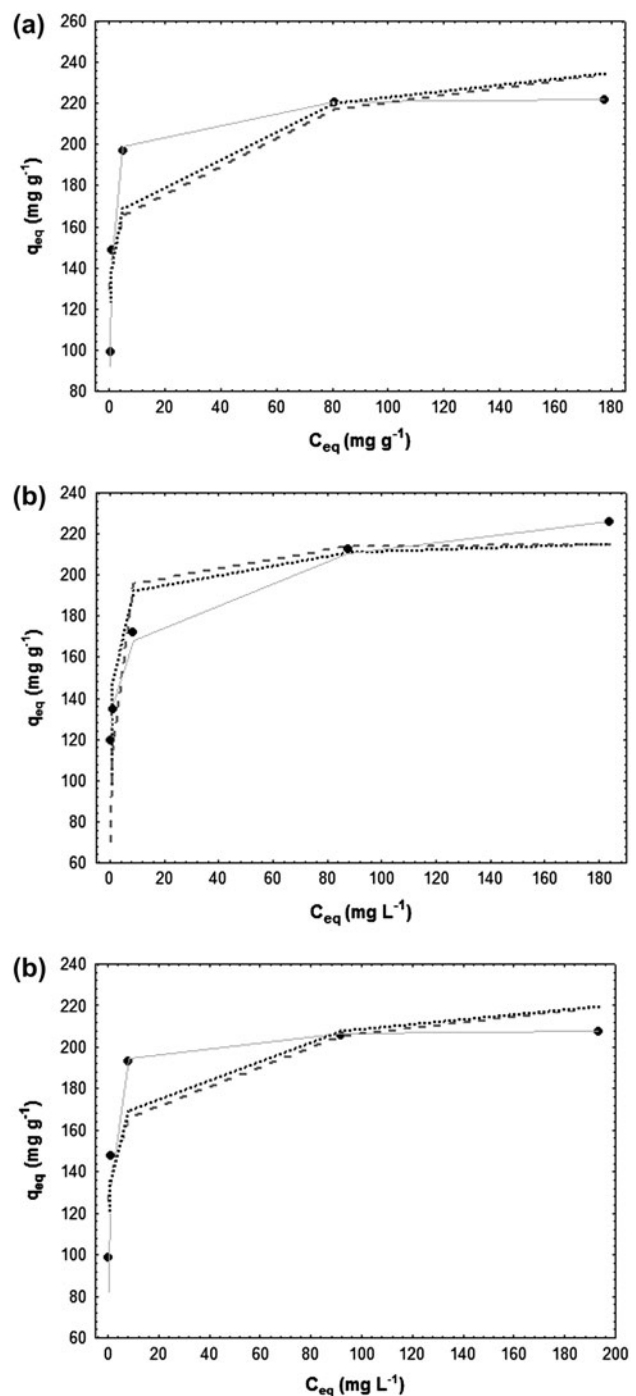


Fig. 9. Bordeaux S dye adsorption equilibrium, experimental data (●) obtained at 20°C (a), 30°C (b), and 40°C (c), and Langmuir (—), Freundlich (---), and Temkin (····) isotherms.

equilibrium studies carried out at 20, 30, and 40°C and pH 2.0. Fig. 9 shows the relationship between the amount of Bordeaux S dye adsorbed per gram of sericin powder (q_{eq}) and the equilibrium concentration

(C_{eq}) at 20 °C (Fig. 9(a)), 30 °C (Fig. 9(b)) and 40 °C (Fig. 9(c)). The maximum Bordeaux S dye adsorption was $222.89 \pm 0.80 \text{ mg g}^{-1}$ at 20 °C, compared with 215.50 ± 0.85 and $207.68 \pm 0.93 \text{ mg g}^{-1}$ at 30 °C and 40 °C, respectively. The results indicated that the amount of adsorbed solute decreased with an increase in temperature, indicating that the adsorption process was exothermic.

The isotherm parameters and statistical analysis are summarized in Table 2. The Langmuir isotherm shows the best fit for all temperatures evaluated at equilibrium, with R ranging from 98.67 to 99.71% and the lowest values for SSR (147–537), and ME (0.15–0.29). The monolayer adsorption process, characteristic of the Langmuir isotherm, is compatible with the specific interaction between some functional groups of the adsorbate; in this case, the sulfonate group of the Bordeaux S dye, and in the adsorbent, the amino acids of the sericin powder have a positive charge in the liquid phase.

The Freundlich and Temkin isotherms, which are typically multilayer adsorption isotherms, predicted adsorption values which differed from the experimental

data, with higher values for EM (0.51–0.66) and SSR (1,349–2,334), as expected since the electrostatic interaction between the Bordeaux S dye and sericin occurs predominantly through an adsorption mechanism, and the interaction between adsorbate–adsorbate molecules is reduced due to the repulsion between the negatively charged sulfonate groups of each molecule.

Table 3 reports the equilibrium thermodynamic parameters, that is, the adsorption equilibrium constant for the Bordeaux S adsorption onto sericin (K_{EQ}), Gibbs free energy (ΔG_{ADS}), and the enthalpy (ΔH_{ADS}) and entropy (ΔS_{ADS}) of adsorption. The ΔG_{ADS} values were negative for all temperatures evaluated in the range of -15.19 to $-13.46 \text{ kJ mol}^{-1}$, which indicates that the adsorption process is spontaneous at pH 2.0, while the ΔH_{ADS} of $-0.27 \text{ kJ mol}^{-1}$ shows that the process is exothermal.

The ΔS_{ADS} value of $+46.12 \text{ J mol}^{-1} \text{ K}^{-1}$ suggests an increase in the randomness at the solid/solution interface with some structural changes in the adsorbate and adsorbent and an affinity between Bordeaux S and the sericin powder, due to the difference between the liquid positive charge at the sericin surface at pH

Table 2

Freundlich, Langmuir, and Temkin isotherm constants; equilibrium parameters and the statistical analysis of Bordeaux S dye adsorption

Isotherm models	Parameters	20 °C	30 °C	40 °C
Langmuir	q_{MAX} (mg g^{-1})	222.52 ± 0.22	215.87 ± 1.09	208.04 ± 0.42
	KL (L mg^{-1})	1.68 ± 0.24	1.16 ± 0.62	1.77 ± 0.61
	SSR	147	455	537
	EM	0.15	0.28	0.29
	R^2	99.71	98.67	99.52
Freundlich	K_F ($\text{L}^n \text{ mg}^{1-n} \text{ g}^{-1}$)	141.34 ± 15.96	136.68 ± 14.10	137.66 ± 14.66
	N	0.098 ± 0.029	0.096 ± 0.026	0.088 ± 0.027
	SSR	2,153	1,597	2,334
	EM	0.59	0.54	0.66
	R^2	80.85	83.85	79.79
Temkin	K_T (L mg^{-1})	$1,919.68 \pm 4,504.06$	$2,316.92 \pm 5,004.15$	$5,357.53 \pm 14,345.12$
	B (J g mg^{-2})	218.90 ± 51.81	239.36 ± 50.57	271.75 ± 66.01
	SSR	1,613	1,349	1,919
	EM	0.51	0.52	0.59
	R	85.60	88.17	84.89

Table 3

Equilibrium constants, standard Gibbs free energy, and enthalpy and entropy of adsorption of Bordeaux S dye onto sericin powder

Temperature (°C)	K_{EQ}	ΔG_{ADS} (kJ mol^{-1})	ΔH_{ADS} (kJ mol^{-1})	ΔS_{ADS} ($\text{J mol}^{-1} \text{ K}^{-1}$)
20	337.53	-14.19		
30	208.41	-13.46	-0.27	+46.12
40	331.67	-15.11		

2.0 and the negative charge of the sulfonate group of the Bordeaux S dye. Moreover, the ΔH_{ADS} value of $-0.27 \text{ kJ mol}^{-1}$ suggests that the adsorption of Bordeaux S dye onto the sericin powder is governed by physical interaction mechanisms, suggesting that electrostatic interaction may be one of the mechanisms involved.

4. Conclusion

The results of this study revealed that sericin powder obtained from the degumming process has good potential for the treatment of aqueous solutions of the dye Bordeaux S. The adsorption process occurred at pH below 3.2, due to the interaction between the positive surface charge of sericin and negative charge of the sulfonate groups of the Bordeaux S dye.

The maximum adsorption rate obtained at equilibrium was $222.89 \pm 0.80 \text{ mg g}^{-1}$ at 20°C and pH 2.0, while an increase in the temperature reduced the adsorption capacity of the sericin. The kinetic and equilibrium study showed fast biosorption and monolayer interaction, with the pseudo-second-order and Langmuir isotherm models providing the best fits. According to the thermodynamic analysis, the adsorption of Bordeaux S dye onto sericin is an exothermic and physical process with electrostatic interaction being the predominant adsorption mechanism.

Acknowledgments

The authors thank Fundação Araucária and CAPES (Brazilian Agencies) for the financial support and scholarship.

References

- [1] B. Zargar, H. Parham, A. Hatamie, Fast removal and recovery of amaranth by modified iron oxide magnetic nanoparticles, *Chemosphere* 76 (2009) 554–557.
- [2] A. Mittal, L.K. Kurup, V.K. Gupta, Use of waste materials—Bottom ash and de-oiled soya, as potential adsorbents for the removal of amaranth from aqueous solutions, *J. Hazard. Mater.* 117 (2005) 171–178.
- [3] C. Fernandez, S. Larrechi, M.P. Callao, An analytical overview of processes for removing organic dyes from wastewater effluents, *Trends Anal. Chem.* 29 (2010) 1202–1211.
- [4] A. Ergene, K. Ada, S. Tan, H. Katircioğlu, Removal of Remazol Brilliant Blue R dye from aqueous solutions by adsorption onto immobilized *Scenedesmus quadricauda*: Equilibrium and kinetic modeling studies, *Desalination* 249 (2009) 1308–1314.
- [5] I. Özbay, U. Özdemir, B. Özbay, S. Veli, Kinetic, thermodynamic, and equilibrium studies for adsorption of azo reactive dye onto a novel waste adsorbent: Charcoal ash, *Desalin. Water Treat.* 51 (2013) 6091–6100.
- [6] A. Srinivasan, T. Viraraghavan, Decolorization of dye wastewaters by biosorbents: A review, *J. Environ. Manage.* 91 (2010) 1915–1929.
- [7] M.T. Sulak, H.C. Yatmaz, Removal of textile dyes from aqueous solutions with eco-friendly biosorbent, *Desalin. Water Treat.* 37 (2012) 169–177.
- [8] Y.Q. Zhang, M.L. Tao, W.D. Shen, J.P. Mao, Y.H. Chen, Synthesis of silk sericin peptides–L-asparaginase conjugates and their characterization, *J. Chem. Technol. Biotechnol.* 81 (2006) 136–145.
- [9] J.H. Wu, Z. Wang, S.Y. Xu, Preparation and characterization of sericin powder extracted from silk industry wastewater, *Food Chem.* 103 (2007) 1255–1262.
- [10] G. Freddi, R. Mossotti, R. Innocenti, Degumming of silk fabric with several proteases, *J. Biotechnol.* 106 (2003) 101–112.
- [11] W. Lamoolphak, W.D. Eknankul, A. Shotipruk, Hydrothermal production and characterization of protein and amino acids from silk waste, *Bioresour. Technol.* 99 (2008) 7678–7685.
- [12] K.J. Park, H.H. Jin, C.K. Hyun, Antigenotoxicity of peptides produced from silk fibroin, *Process Biochem.* 38 (2002) 411–418.
- [13] Y.Q. Zhang, Applications of natural silk protein sericin in biomaterials, *Biotechnol. Adv.* 20 (2002) 91–100.
- [14] B.C. Dash, B.B. Mandal, S.C. Kundu, Silk gland sericin protein membranes: Fabrication and characterization for potential biotechnological applications, *J. Biotechnol.* 144(4) (2009) 321–329.
- [15] F.R.B. Turbiani, J. Tomadon Jr, F.L. Seixas, M.L. Gimenes, Properties and structure of sericin films: Effect of the crosslinking degree, *Chem. Eng. Trans.* 24 (2011) 1489–1494.
- [16] A. Takeushi, C. Ohtsuki, T. Miyazaki, M. Kamitakahara, S. Ogata, M. Yamazaki, Y. Furutani, H. Kinoshita, M. Tanihara, Heterogeneous nucleation of hydroxyapatite on protein: Structural effect of silk sericin, *J. R. Soc. Interface* 2 (2005) 373–378.
- [17] C. Fan, J. Li, G. Xu, H. He, X. Ye, Y. Chen, X. Sheng, J. Fu, D. He, Facile fabrication of nano-hydroxyapatite/silk fibroin composite via a simplified co-precipitation route, *J. Materials Sci.* 45 (2010) 5814–5819.
- [18] M.L. Gimenes, L. Liu, X. Feng, Sericin/poly(vinyl alcohol) blend membranes for pervaporation separation of ethanol/water mixtures, *J. Membr. Sci.* 295 (2007) 71–79.
- [19] R.F. Weska, W.C. Vieira Jr, G.M. Nogueira, M.M. Bepu, Effect of freezing methods on the properties of lyophilized porous silk fibroin membranes, *Mater. Res.* 12 (2009) 233–237.
- [20] M.A.A. Aslani, M. Eral, S. Akyil, Separation of thorium from aqueous solution using silk fibroin, *J. Radioanal. Nucl. Chem.* 238 (1998) 123–127.
- [21] X. Chen, K.F. Lam, S.F. Mak, K.L. Yeung, Precious metal recovery by selective adsorption using biosorbents, *J. Hazard. Mater.* 186 (2011) 902–910.
- [22] V.R. Silva, M. Ribani, M.L. Gimenes, A.P. Scheer, High molecular weight sericin obtained by high temperature and ultrafiltration process, *Procedia Eng.* 42 (2012) 833–841.
- [23] B. Sethi, S. Jyoti, Kinetic study of steam activated pigmented rice husk carbon as an adsorbent to remove

- amaranth dye from aqueous solution, *Novel Sci. Int. J. Pharm. Sci.* 1 (2012) 83–86.
- [24] S. Brunauer, P.H. Emmett, E. Teller, Adsorption of gases in multimolecular layers, *J. Am. Chem. Soc.* 60 (1938) 309–319.
- [25] A. Salis, M. Boström, L. Medda, F. Cugia, B. Barse, D.F. Parsons, B.W. Ninham, M. Monduzzi, Measurements and theoretical interpretation of points of zero charge/potential of BSA protein, *Langmuir* 27 (2011) 11597–11604.
- [26] Y.S. Ho, G. McKay, Pseudo-second order model for sorption processes, *Process Biochem.*, 34 (1999) 451–465.
- [27] H. Qiu, L.V. Lu, B.C. Pan, Q.J. Zhang, W.M. Zhang, Q.X. Zhang, Critical review in adsorption kinetic models, *Zhejiang. Univ. Sci. A* 10 (2009) 716–724.
- [28] P.R. Puranik, J.M. Modak, K.M. Paknikar, A comparative study of the mass transfer kinetics of metal biosorption by microbial biomass, *Hydrometallurgy* 52 (1999) 189–197.
- [29] D.M. Ruthven, *Principles of Adsorption and Adsorption Process*, Wiley, New York, NY, 1984.
- [30] A.A. Khan, R.P. Singh, Adsorption thermodynamics of carbofuran on Sn (IV) arsenosilicate in H^+ , Na^+ and Ca^{2+} forms, *Colloids Surf.* 24 (1987) 33–42.
- [31] S. Da Ros, G. Colusso, T.A. Weschenfelder, L.M. Terra, F. Castilhos, M.L. Corazza, M. Schwaab, A comparison among stochastic optimization algorithms for parameter estimation of biochemical kinetic models, *Appl. Soft Comp.* 13 (2013) 2205–2214.
- [32] K.H. Lee, G.D. Kang, B.S. Shin, Y.H. Park, Sericin-fixed silk fiber as an immobilization support of enzyme, *Fibers Polym.* 6 (2005) 1–5.